Peel-Strength Behavior of Bilayer Thermal-Sprayed Polymer Coatings

F. Y. Yan,[1,2] K. A. Gross,[1] G. P. Simon,[1] C. C. Berndt[3]

[1]*School of Physics and Materials Engineering, P.O. Box 69M, Monash University, Victoria 3800, Australia*
[2]*State Key Laboratory of Solid Lubrication, Lanzhou Institute of Chemical Physics, Chinese Academy of Sciences, Lanzhou 730000, People's Republic of China*
[3]*Department of Materials Science and Engineering, State University of New York at Stony Brook, Stony Brook, New York 11794-2275*

Received 27 November 2001; accepted 4 June 2002

ABSTRACT: We prepared various bilayer polymer coatings of ethylene methacrylic acid (EMAA) copolymer and ionomer by the thermal-spray process under a range of preheat temperatures (PTs) to investigate their ability to be repaired. The thermal properties, crystallinity, microstructure, and interface strength of the coatings were investigated with differential scanning calorimetry, X-ray diffraction, scanning electron microscopy, and mechanical testing. Processing parameters influenced the final morphological structure of the coatings. The crystallinity of the coatings increased with a higher final temperature, whereas the coating density decreased. The decrease in density was attributed to the appearance of bubbles, 250 μm in size, formed in the coatings during the spray process. For the monolayer coating of polymer on a metal substrate, a higher PT produced a greater contact area of the coating to the substrate. The adhesion of EMAA ionomer to steel was always lower than that of EMAA copolymer to steel. This may have been largely due to the interfacial adhesion between the polymer and steel being dominated by strong secondary bond interactions. Experimental results also indicate that the peel strength between polymers was at least twofold stronger than that between the polymer and the steel substrate for PTs greater than 100°C. The mixed bilayer coating of ionomer on copolymer produced the highest peel strength. The interface between the plastic layers was clearly visible under the scanning electron microscope at lower PTs, becoming more diffuse with an increase in PT. On the basis of these observations, the adhesion mechanism between polymers was explained by the formation of welding points. J Appl Polym Sci 88: 214–226, 2003

Key words: coatings; adhesion, strength; structure–property relations

INTRODUCTION

Plastic coatings have been used widely for improving the strength of glass bodies,[1] surface decoration, corrosion protection,[2,3] and wear resistance.[4,5] These applications include the lining of vessels in the chemical industry, coatings on light poles, and coatings on bridges for environmental protection. Coupled with metal or ceramic powders, plastics work well for abrasion applications in the aviation industry,[6] for antislip surfaces for safe pedestrian use on steps,[7] or in factories where walking surfaces may become wet.

Various technologies are available for the deposition of plastic coatings, ranging from painting, powder coating, and thermal spraying. Painting releases volatile organic solvents and, therefore, is not an environmentally sound option. Powder coating, although effective in coating large surfaces, is fixed to the location of large baking ovens. Thermal spraying is a widely used technique[8–10] and presents a low-cost, low-pollution option that uses simple equipment and procedures. Large defective areas on the sprayed surface can be repaired simply by the application of a new coating.[11,12] The low softening temperature of polymers allows the coating of polymer-based materials and traditional metals and ceramics.

The thermal spraying of plastics involves the powder injection of a polymer powder into a flame followed by deposition onto a surface. A powder with an average particle size of about 200 μm is fed from a fluidized bed powder feeder and is injected axially into a flame. Gases for flame spraying include combustion gases such as acetylene, propane, propylene, and hydrogen together with either air or oxygen.[13] Among the various gases available, acetylene and propane are the most commonly used. The powder is injected into the flame, where the particles are accelerated to about 60 m/s.[14] During their traverse in the flame, the particles pass through a peak temperature at the spray-torch nozzle exit that decreases both axially and radially. This thermokinetic history is suffi-

Correspondence to: K. A. Gross (karlis.gross@spme.monash.edu.au).

Contract grant sponsor: NSF INT; contract grant number: NSF INT 9513462.

cient to rapidly heat, soften, and melt the polymer powder.[15] After traveling a distance of 30 cm, the particles are usually sufficiently well softened and are collected onto a substrate. The substrate is typically roughened by grit blasting to enhance the coating adhesion. The gun is rastered across the substrate to deliver a succession of molten droplets to build up a coating. Continuous rastering of the flame-spray torch dictates the thickness of the coating that is produced. Other heat sources, such as a plasma or a high-velocity flame, may also be used for the generation of plastic coatings, but these processes are not the subject of this article.

A number of authors have reported the effects of thermal-spray processing parameters on the resulting polymer coatings on metal substrates.[9,10] Physical models describing the formation of combustion-sprayed polymer coatings have been developed based on the concepts of classic particle coalescence and the dynamics of deposit formation.[14,16] These models all aid in the understanding of the underlying principles of thermal spray and the improved application of the technique.

The history of thermal spray indicates that emphasis was initially placed on *reclamation*, that is, a process of refurbishing a worn surface, which was then restored to the original dimensions by thermal spraying.[17] Today, coatings may be damaged in service and may require a small repair or recoating of the entire surface. The more common response to this situation has been to remove the coating by water blasting or chemical treatment or with a mechanical operation. Plastic materials do not exhibit residual stress, such as in high-elastic-modulus materials, metals, and ceramics, and may be more easily repaired by the addition of a second coating.

Because the polymer coatings can be repaired by a simple reapplication of the same or similar materials to the desired location, bilayer coatings need to be optimized before application in real industrial situations. Therefore, it is important to understand the interface cohesion behavior of bilayer polymer coatings and the factors that influence their properties. To date, attention has mainly been given to the study of mechanical and adhesion properties and the processing effects of monolayer plastic coatings on steel substrates. Nothing has been reported about the factors that influence the adhesion of bilayer coating systems. Thus, the objectives of this work were (1) to study the structures and mechanical behavior of bilayer coatings of various polymer pairs and (2) to understand the influence of the preheat temperature (PT) of substrates on the interfacial cohesion between polymers to provide insight into the repair of coatings.

The range of polymers that have been used as coatings include nylon, polyethylene,[18] polyamide,[19] polymethylmethacrylate,[20] PEEK,[21] and ethylene methacrylate acid copolymers.[14] Thermoplastic materials of ethylene methacrylic acid (EMAA) copolymer and its ionomer, containing Na^+ ions, are the most commonly used polymers in the flame-spray process. This polymer adheres exceptionally to steel surfaces and can be applied in high humidities and at temperatures below the freezing point.[22–24] The thermal-spray process parameters and coating properties of EMAA have been determined systematically by various methods.[25–27] In this work, two polymeric materials with similar molecular structures and chemical and physical properties were used, and coating properties both on steel and in bilayer spraying (polymer-on-polymer) were examined.

EXPERIMENTAL

Coating production

Two dehydrated commercial powders of EMAA copolymer (PF111U, 70 mesh) and a Na^+-containing ionomer (PF112U, 80 mesh), provided by Plastic FlameCoat Systems (PFS Thermoplastics, Big Spring, TX), were used in this study. NMR studies using ^{13}C cross-polarity/magic-angle-spinning NMR spectroscopy indicated that these copolymers are random copolymers with 7% methacrylic monomer and 93% ethylene. The full details of the chemical and physical properties of the EMAA copolymer and ionomer are described elsewhere.[23–27] A Powder Pistol 124 from PFS was used both for preheating the substrate and for spraying the coating. Propane (at 12 psi) and compressed air (at 80 psi) were used to produce the combustion flame; the compressed air was also used to fluidize the powders and transport the powders from the fluidized bed to the torch. The principle of the plastic flame-spray system deposit EMAA coatings and various process parameters were described previously.[25–27] PT and final coating temperature (FCT) were measured with a handheld IR pyrometer for several seconds after spraying. In this work, FCT was controlled by variation of the traverse interval of the spray torch during processing.

PF111 and PF112 polymer coatings were deposited onto a poly(tetrafluoroethylene) (PTFE)-coated aluminum plate (thickness = 3 mm, diameter = 250 mm) preheated to 80°C to prepare one large coating from which samples were taken for density, differential scanning calorimetry (DSC), X-ray diffraction (XRD), and tensile testing measurements.

Other coatings for peel-strength testing were deposited onto carbon steel bars (length = 190 mm, width = 25 mm, thickness = 10 mm). The surface of the steel bar was cleaned with acetone before spraying. According to the requirements of the peel test, one prepeeled section of a coating with a given length on the sample surface was required. In our initial work, the

TABLE I
Densities of Coatings Manufactured at Different FCTs in Comparison with the Source Powder

	Powder (g/cm^3)	Coating (g/cm^3)			
		210°C	230°C	260°C	290°C
PF111 copolymer	0.9392 ± 0.0008	0.9378 ± 0.0005	0.9375 ± 0.0005	0.9360 ± 0.0003	0.9210 ± 0.0006
PF112 ionomer	0.9636 ± 0.0008	0.9537 ± 0.0007	0.9527 ± 0.0005	0.9519 ± 0.0004	0.9467 ± 0.0006

normal antistick method of using a PTFE dry film, as used for polymer/steel samples, was shown not to be suitable for the polymer/polymer interface. Thus, an antistick method, as described next, for bilayer-polymer-coating samples was developed in this study. The first polymer layer was thermal sprayed and allowed to cool. Then, a very thin graphite film was coated on one end of the coated substrate surface. This was followed with an organic PTFE dry film on the section to achieve a more ideal antistick effect. The peel test samples with an EMAA bilayer coating could, therefore, be prepared by the thermal-spray process.

Powder and coating characterization

Density

The densities of powders and coatings were determined with a helium gas pycnometer (AccuPyc 1300, Micromeritics, Norcross, GA) at test conditions of five purges and 15 runs, all at room temperature (20°C). We viewed the 15 measurements separately to ascertain the reproducibility of the densities, and an average was determined.

DSC

We used DSC to determine the melting and crystallization temperatures of the polymers. DSC measurements were conducted at a scanning rate of 10°/min from 25–400°C on a Pyris 1 differential scanning calorimeter (PerkinElmer) in a nitrogen atmosphere with an indium and zinc standard. About 10 mg of each sample was used for the measurements.

XRD

XRD patterns were obtained with a Rigaku Geigerflex diffractometer, with Cu K α, radiation at 22.5 mA and 40 kV passing through a 0.3° receiver and a 0.5° divergence slit. A scan rate of 1°/min and a step size of 0.05° were selected over a 2θ range of 1.5–35°.

Scanning electron microscopy (SEM)

Surface images and fracture cross-sections of polymer coatings were observed on a Jeol JSM-840A scanning microscope. To prevent deformation of the polymer coatings at normal temperature, we immersed samples in liquid nitrogen and then removed and immediately fractured them. Sputter coating was performed with a gold target over a period of 1 min with cycles that involved a 4-s coating time and a 4-s resting time. This ensured that the polymer was not overheated during sample preparation. Accelerating voltages of 15–20 kV were used during SEM observations.

Mechanical testing

Tensile testing

Tensile test samples were produced by spraying onto a Teflon-coated substrate from which they could be readily removed. A stamping tool was then used to form dog-bone-like samples 25 mm in length, 3.5 mm in width, and about 1 mm in thickness. Tensile testing was conducted on an Instron 4505 mechanical testing system at a crosshead speed of 50 mm/min and at room temperature (~20°C). A minimum of five samples were tested for each condition to assess variations in coating properties. The modulus was calculated automatically with a secant modulus at 1% strain. The yield stress was determined from the stress–strain curve. The tensile strength was defined as the maximum stress obtained from the curve.

Peel-strength testing

Adhesion of the polymer coating to mild steel (monolayer configuration) or on a previously sprayed layer (bilayer configuration) was determined with a 90° peel test rig. The coating thickness for the monolayer samples was about 1 mm, but bilayer samples were about 2 mm thick to accommodate the base and top layer. The peel test was also conducted on the Instron 4505 mechanical testing system at a peel speed (crosshead speed) of 50 mm/min. A minimum of four samples was tested for each condition.

RESULTS AND DISCUSSION

Basic characteristics of the sprayed samples

Table I shows the densities of PF111 and PF112 powders and their coatings. We prepared the coating samples by thermally spraying molten plastic powders onto Teflon-coated substrates at a PT of 80°C and at various FCTs. FCT was controlled by variation of the

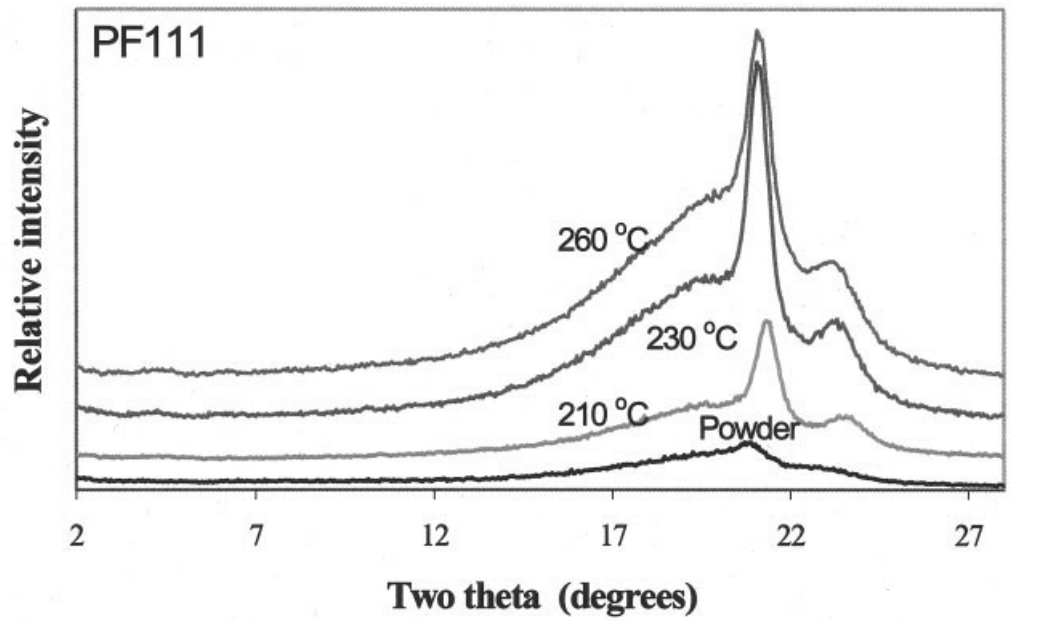

(a)

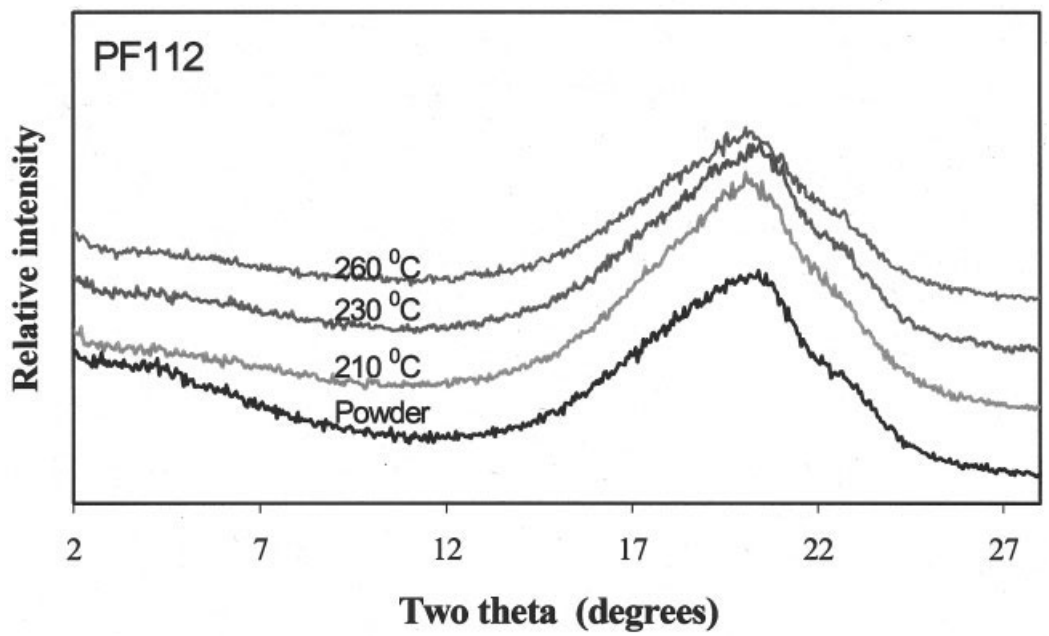

(b)

Figure 1 XRD patterns of (a) PF111 and (b) PF112 powders and coatings. FCTs were 210, 230, and 260°C, as shown.

time between traverses of the spray pistol. The shorter time delay between traverses produced a higher FCT. Table I indicates that the density of the powder was always higher than that of the coating. An increase in coating temperature produced a low coating density. The XRD results shown in Figure 1 indicate that both EMAA powders contained amorphous and crystalline components. The coatings exhibited an increase in crystallinity with higher FCT. There were two factors that could have influenced the density value of the

material: (1) the change in material crystallinity after the melting and recrystallizing processes and (2) the appearance of air bubbles due to degradation and polymer oxidation at the relatively high temperatures. An increase in porosity appeared to be the dominating factor.

As the maximum temperature of a propane/compressed air flame is about 1300°C[28] and particles traverse quickly through the flame, some degradation and oxidation of the polymer is possible during thermal-spray processing, which may lead to a slight increase in coating porosity. The porosity appeared to increase with temperature. A more rapid decrease in coating density occurred when the final temperature was above 260°C. Above that temperature, the color of the coating changed from transparent to an opaque light yellow, and many bubbles were observed in the coating. This temperature may have been the so-called second temperature threshold proposed by Brogan,[14] although in this study, it was found to be above 216°C. The first temperature threshold mentioned was the minimum temperature required to coalesce polymer particles by viscous flow for maximum density. The second temperature threshold promoted diffusion at the splat boundaries so that boundaries were no longer discernible. It has been reported that gaseous products are liberated if coatings are sprayed beyond this second temperature threshold, thereby decreasing strength, toughness, and hardness.[14] It should be stressed that although some limited discoloration and volatilization occurs, the change in molecular structure is minimal when the high temperatures in the process are considered,[26] and the polymer generally retains its mechanical integrity.

Typical DSC curves are shown for the two powders, PF111 and PF112, and the coatings sprayed at different FCTs in Figure 2(a,b). In the case of PF111 [Fig. 2(a)], two main features were seen. The lower temperature transition was the glass-transition temperature, at about 55°C for the neat powder, as shown in Table II. This appeared to move to slightly lower temperatures when PF111 was flame sprayed. A higher coating temperature decreased the glass-transition temperature. This may have been due to a slight degradation of the chains during coating and possibly to a change in morphology due to the crystal structure leading to a less constrained amorphous region, surrounded by crystallites. The data also showed an endothermic overshoot, indicative of physical aging just below the glass transition. However, this dependency is unclear in Figure 2(a) because the sample where the powder had not been exposed to annealing during cooling from the spray temperatures showed the largest overshoot. Some level of aging could have occurred during synthesis and processing of the polymer into the powders eventually used for coatings. The high-temperature peak of PF111 in Figure 2(a) at about 90–100°C was clearly related to the melting of crystallites and appeared broad, with multiple melting peaks underlying it. This could have been due to the melting and recrystallization phenomena of the samples during the DSC run. Nonetheless, on the basis DSC results, it would seem that the crystallinity of PF111 did not vary substantially between powder and coating. In this sense, the DSC technique was not as able to discriminate crystallinity as could XRD, as shown in Figure 1(a,b).

As seen in the broad XRD patterns for the powder and coatings of PF112 in Figure 1(b), Figure 2(b) also indicates unusual behavior. A glass-transition type of response decreased from around 55°C for the powder to 45°C for the sample with an FCT of 260°C. Unusually, the 210°C coating had a large endothermic aging overshoot. The melting endotherms at 90°C were quite broad, and their area (and, hence, endothermic energy) did not follow a clear trend. The similarity between these materials is reflected by the X-ray data in Figure 1 (b), which shows that the crystallinity was lower in PF112, as expected, due to its ionomeric nature and interchain interactions, which decreased the crystallinity of the ethylene copolymer units.

The tensile properties of polymers have a direct relationship with the processing conditions.[27] The FCT appears to be a very important parameter influencing the tensile properties of coatings. Table III shows the tensile test results of the polymer coatings sprayed directly onto a PTFE substrate (for ease of removal). Both strain at failure (ductility) and the maximum stress of coating increased with an increase in FCT; whereas the 1% secant modulus decreased. These results matches well with those available in the literature.[14,27] It can be concluded that to achieve optimal particle coalescence, a higher final processing temperature close to the second threshold temperature is necessary, provided that this does not lead to excessive degradation and oxidation. On the basis of these results, we considered that the optimized FCT should be at about 230°C.

Because the temperature of the deposited thermoplastic coating depended on the substrate PT, gun traverse speed, and other parameters, it was necessary to vary the time between traverses frequently during spraying to control the FCT at a constant traverse speed. The FCT of the sprayed samples described later was controlled to about 230°C.

Monolayer thermal-sprayed coatings

In this section of study, peel tests were mainly used to evaluate the interfacial cohesion for both monolayer and bilayer coatings. As a first step, the influence of coating thickness on the peel strength was determined because no data, to the best knowledge of the authors, was available for thermoplastic sprayed coatings. The

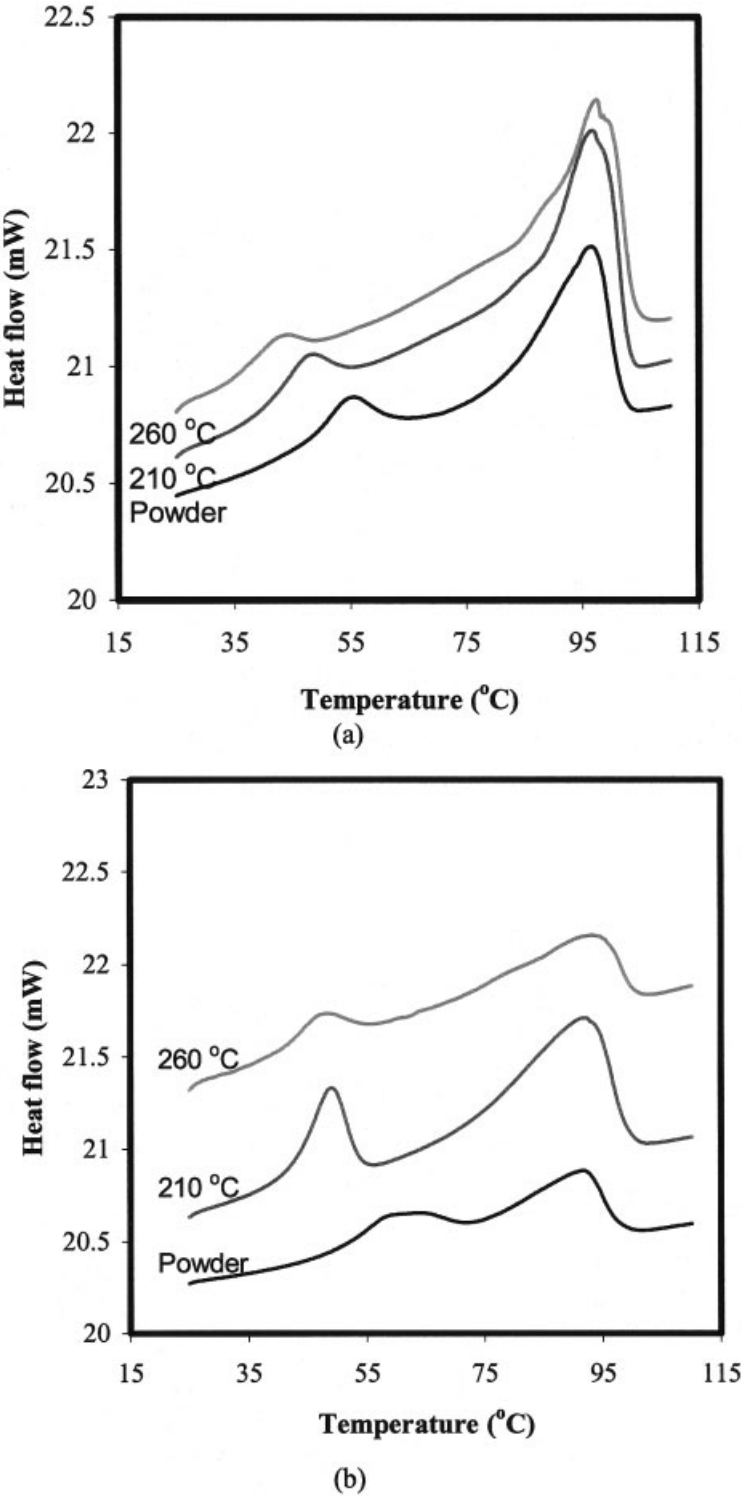

Figure 2 DSC curves of PF111 and PF112 powders and coatings. FCTs were 210 and 260°C, as shown.

peel strength of PF111 coatings was determined for thicknesses from 0.5 to 2 mm, tested at a crosshead speed of 50 mm/min. The PT of the carbon steel substrate and the FCT in this case were 100°C and about 230°C, respectively. An increase in coating thickness led to a slight decrease in the peel strength, which was almost constant in the thickness range of 0.5–2 mm, Figure 3. The results also indicate that the coating/substrate interface behavior was dominated mainly by material factors, surface properties such as cleanliness and roughness, and conditions of the interface before spraying. The interface behavior was relatively stable despite the continuous deposition of molten polymer particles, which caused a different

TABLE II
Thermal Properties of PF111 and PF112 Powders and Coatings

		T_g (°C)	ΔH_1 (J/g)	T_m (°C)	ΔH_h (J/g)
PF111	Powder	54.78	10.15	96.27	37.31
	Coating at 210°C	47.60	4.62	96.55	51.86
	Coating at 260°C	42.66	2.74	97.39	50.77
PF112	Powder	58.89	12.34	91.62	19.35
	Coating at 210°C	48.93	11.74	91.76	38.95
	Coating at 210°C	46.95	7.19	92.90	36.97

thermal history for coatings of different thicknesses, and an accompanying stress distribution within the coating. Thus, in this study, the influence of coating thickness on the peel test results could be ignored, although effort was made to maintain a similar thickness for all coatings.

The variation of the peel strength of the monolayer coatings as a function of different PTs of the mild steel substrates was also determined, as shown in Figure 4. The final temperature of all coatings was set to about 230°C by variation of the traverse interval of the spray torch. The peel strength of the sprayed monolayer coatings continuously increased with PT from room temperature to 140°C. In addition, for the same PT of the steel substrate and other processing parameters, the peel strength of the ionomer, PF112, was always lower than that of the copolymer, PF111. It was assumed that the interface adhesion between the polymer coating and steel substrate was dominated by physical adsorption because of secondary bonding by the polar methacrylic acid copolymer and the very-high-energy metal. The reason that the ionomer was less adhesive was possibly due to the association of Na^+ ions with the methacrylic acid in secondary bonds, which formed a physically crosslinked superstructure and, thus, were not available to interact strongly with the metal.[23,24]

The relationship between peel strength and PT can be explained with reference to the coating-formation process, which can be interpreted as a successive stacking of molten particles.[8,14] When particles first contact the substrate surface, heat exchange between particles and the substrate will occur because of the temperature difference. It is likely that the mode and kinetics of heat exchange will influence the adhesive strength between the coating and substrate, manifesting as peel strength. It has been widely accepted that because the preheat vaporizes any trapped water and allows the molten particles to flow into the substrate topography, a higher substrate PT and a longer cooling time are important prerequisites for the achievement of a stronger interface.[14]

Porosity was an important parameter affecting the coating contact surface area on the metal substrate. The contact area also increased with the substrate PT. Figure 5 shows secondary electron images of the underside of the PF112 coatings (the contact surface of PF112 coatings with metal). No plastic debris was observed on the substrate surface for coatings prepared at low PTs. At PTs lower than the melting point of the polymer (96.3°C for PF111 and 91.6°C for PF112), the peeled surface of the coating appeared smooth with many holes. An increase in PT resulted in a higher surface roughness on the peeled coating. Furthermore, these defects were few and were smaller in size. The roughness of the coating underside reflects the degree of coating adhesion with the substrate; the rougher the underside is, the greater is the interfacial adhesion.

The appearance of defects or pores at the polymer/substrate interface was attributed to the coating-formation process. This was related to the lower temperature threshold mentioned earlier.[14] When the final temperature is lower than this first threshold, poor particle coalescence leads to many holes. When molten or semimolten particles are sprayed from a flame torch and deposited onto a cold substrate, the droplets are rapidly quenched by the relatively cold substrate and solidify to form overlapping splats. If the processing temperature is below the first threshold temperature, the solidification rate is faster, and the droplets do not have sufficient time to spread on the substrate. A uniform thin film cannot be formed, and many defects remain on the substrate. Further splats cannot completely fill the uncovered holes, and thus, porosity at the interface is formed, as seen in Figure 5. With the continuous stacking of polymer splats, the rate of heat loss continues to decrease because of the poor thermal conductivity of polymer coatings,[29] and the molten polymer droplets strike a warmer substrate, thereby retaining sufficient heat to flow or spread on the coated surface. For this reason, the holes are observed predominantly at the interface and not in the middle of the coating.

The formation of such surface flaws is also possible from the volatilization of matter absorbed on the sub-

TABLE III
Tensile Properties of PF111 and PF112 Coatings

	Final temperature (°C)	1% secant modulus (MPa)	Strain at fracture (%)	Tensile strength (MPa)
PF111	210	260	576	12.88
	230	196	612	12.60
	260	179	690	14.07
PF112	210	236	555	19.14
	230	197	633	22.39
	260	181	638	21.63

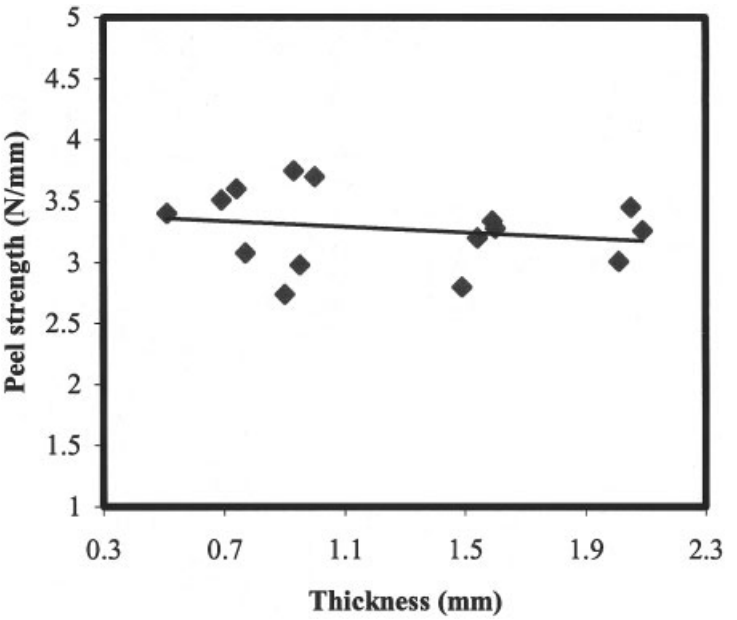

Figure 3 Relationship between the peel strength and flame-sprayed PF111 coating thickness (PT = 100°C, FCT = 230°C).

strate, such as water vapor and organic residue. When the PT is sufficiently high, such as over 60°C for PF111 and PF112, most of the absorbed matter on the substrate surface is evaporated by the flame, whereas the molten polymer splats retain sufficient heat to flow and intermingle with other splats on the substrate surface. In this case, no visible flaws could be formed at the interface between the polymer coating and substrate. The holes are different from the bubbles that form because of the oxidation of the polymer material. Such bubbles, when they occur, have a smoother shape, as shown in Figure 6.

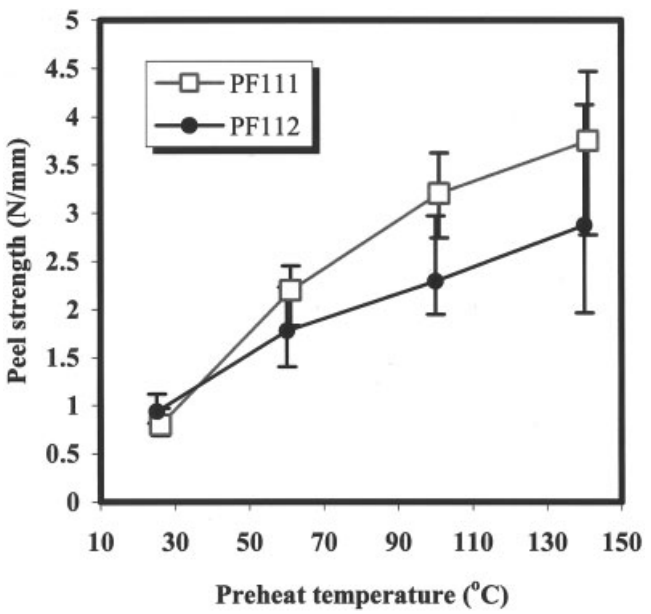

Figure 4 Peel strength of the coatings at different PTs (FCT = 230°C).

Bilayer thermal-sprayed coatings

One of the potential advantages of this processing method is that damaged coating surfaces can be repaired by the same thermal-spray technique with

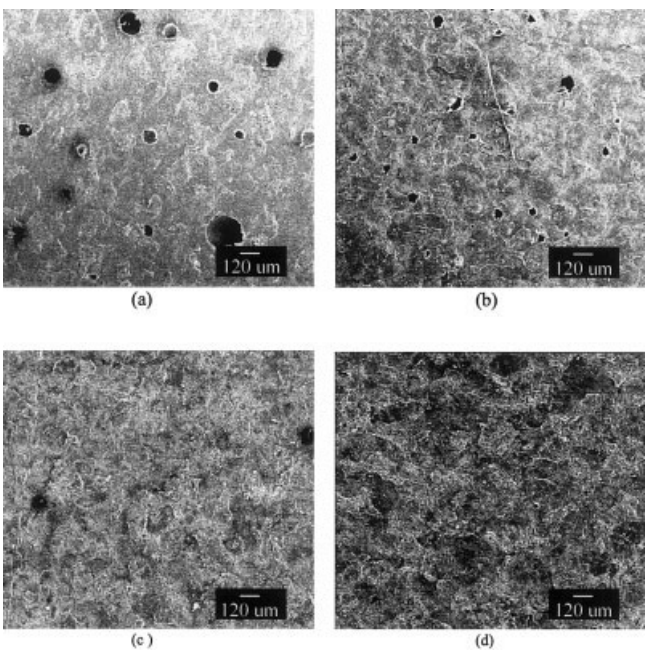

Figure 5 Secondary electron images of PF112 coatings after peel-strength testing. Coatings were preheated to (a) room temperature, (b) 60°C, (c) 100°C, and (d) 140°C (FCT = 230°C).

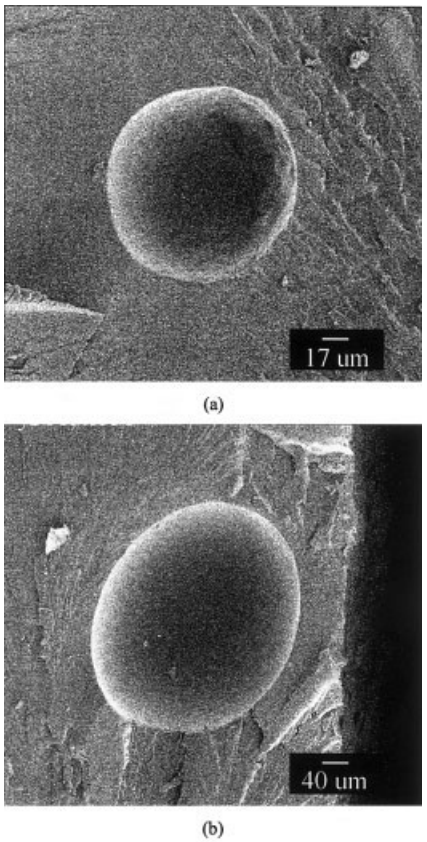

Figure 6 Cross-section of a (a) small void and (b) large void inside a PF112 coating (PT = 100°C, FCT = 230°C).

identical or compatible materials. It is necessary to understand the mechanical behavior of bilayer coatings. To date, there is little in the literature concerning the adhesion of a second layer to a previously sprayed polymer coating. In this study, the interfacial adhesion between the first and the second layers was determined by peel testing. Because peel strength has no obvious relation to coating thickness, the thickness of the first layer was designed to be about 0.3–1.0 mm, with the second layer at about 1.5–2.5 mm. A number of experiments, not included here, proved that this design produced reproducible results.

The peel strength of the top coating exhibited similar force characteristics to those obtained with a single layer, as shown in Figure 7(a). After an initial linear increase in force, an oscillating value of force was established for continued peeling about a mean value. The peeling occurred ahead of the PTFE roller. An analysis of the failure location with a digital video apparatus revealed that larger oscillations could be related to the formation and fracture of microfibrils, as shown in Figure 7(b). The extension of fibrils was related to an increase in peel force because these areas reinforced the peel resistance as the crack location progressed further along the interface.

There are many possible parameters that may influence the interfacial strength, including processing parameters, chemical or mechanical treatment, and degradation of the first coated surface. To allow direct comparison with the mechanical properties of monolayer coating systems, we investigated only the influence of PT (before spraying the second layer) on peel strength of bilayer systems with different layer arrangements of PF111 and PF112. After the first layer was deposited at the same conditions, with a PT (on the steel substrate) of 100°C and a final temperature of about 230°C, 24 h were allowed for the layer to cool and eliminate any stresses in the sprayed coatings. After this, the second layer was deposited at a different PT (on the substrate with first layer) at room temperature and 60, 100, and 140°C. The final temperature used for the second layer was about 230°C for all of the coatings. The peel test results are shown in Figure 8. An increase in PT for PF111 and PF112 bilayer coatings resulted in an increase in the peel strength of the bilayer coatings, which eventually plateaued when the PT was higher than the melting point, as shown in Figure 8(a). The peel strength of the PF111-on-PF111 bilayer coating was lower than that the PF112-on-PF112 bilayer coating. It appeared that under the conditions used, the PF112 may have allowed better indiffusion between the first and second layer. Alternately, the strength for a given interpenetration was greater for the ionomer (PF112) than for the copolymer (PF111). It is possible that the ionomeric superstructure formed ensured good adhesion between the ionomeric species.

It was of interest to determine how the spraying of dissimilar polymers influenced adhesion, that is, PF111 on PF112 and PF112 on PF111. The results of such mixed bilayer systems for various first-layer preheats are shown in Figure 8(b). For mixed PF111 and PF112 bilayer coatings, the peel strength of PF111 on PF112 increased linearly with the PT. However, for PF112 on PF111, the highest peel strength was found for samples with a PT of 60°C. Furthermore, the peel strength of PF112 on PF111 was much greater than that of PF111 on PF112, even under the preparation conditions at room temperature. To date, the reason is not clear. Many factors, such as the oxidation or degradation of the first coated surface, heat exchange modes, melting points and viscosities, and rate of diffusion of both materials, may have affected the final results.

The ionomer, PF112, was better suited to repairing coatings because the peel strength of PF112 on PF112 and PF112 on PF111 was stronger than that of PF111 on PF111 and PF111 on PF112. This result occurred despite the weak adhesion of PF112 onto a steel substrate in comparison to the PF111 coating on steel. The superior adhesion still requires further study. The corollary to this result is that the use of the same polymer material for repair may not provide the best result.

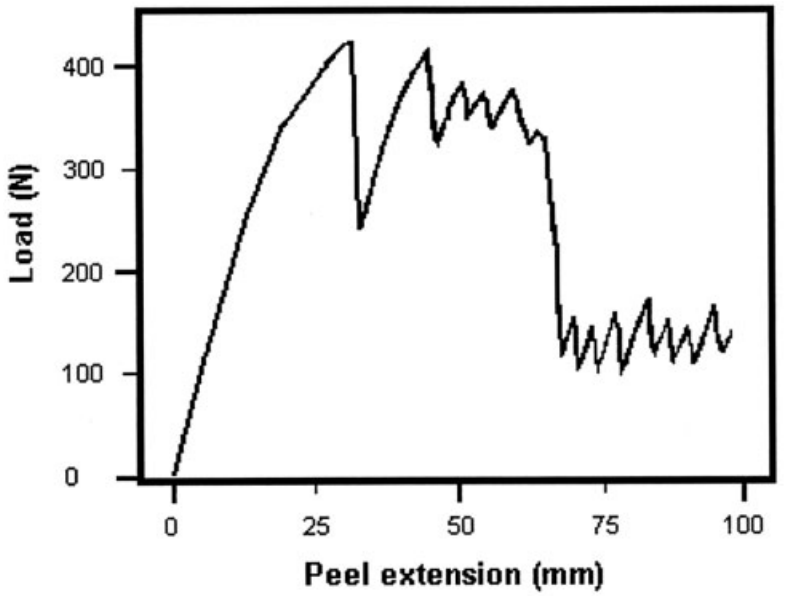

(a)

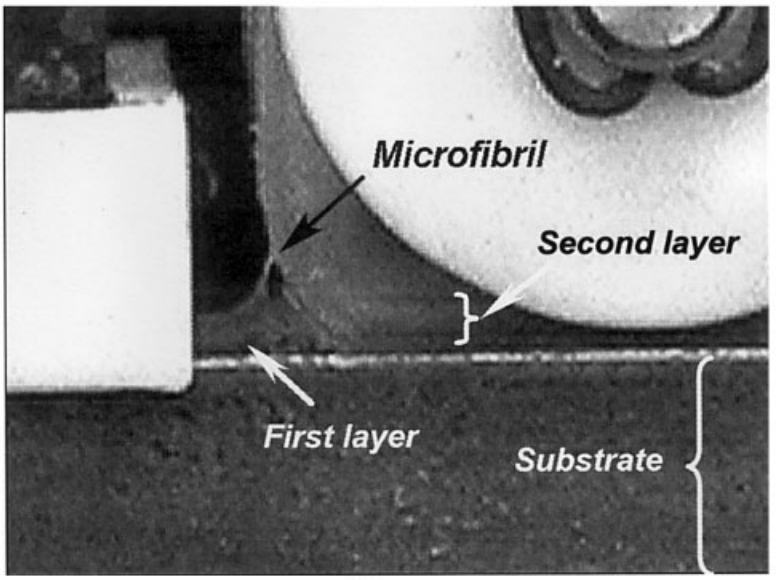

(b)

Figure 7 Typical peel-strength behavior obtained in (a) a load versus peel distance curve and (b) the progressing crack front in a bilayered coating (PF112 on PF111), showing the formation of a microfibril between the metallic substrate and the peeled coating (first layer: PT = 100°C, FCT = 230°C; second layer: PT = 100°C, FCT = 230°C). The height of the white Teflon block to the left was 20 mm.

When the peel strengths of monolayer coatings and bilayer coatings are compared at the same conditions, the strength of bilayer coatings was usually two to five times higher than that of monolayer coatings. Such a result could be attributed to microfibril formation and interlayer diffusion, as discussed previously. It is believed that if the top layer were exposed to conditions that lead to contamination, weathering and degradation, the peel strength of the bilayer coatings may also decrease, and the interfacial adhesion of bilayer coatings may remain higher than that of monolayer coating. This would be the case, for example, where a coating is sprayed and left exposed to the environment for some time before repair. We intend to carry out further work on this aspect.

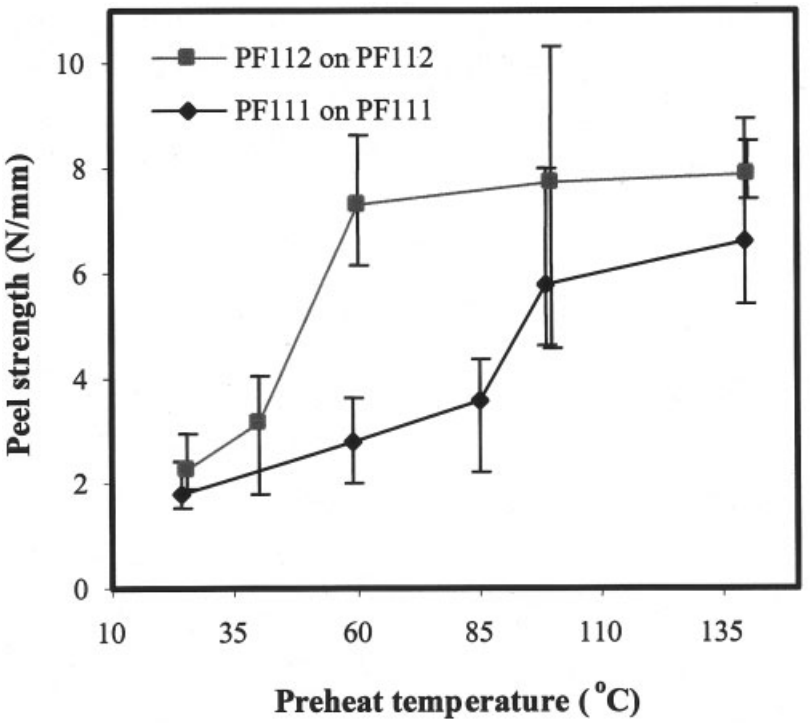

(a)

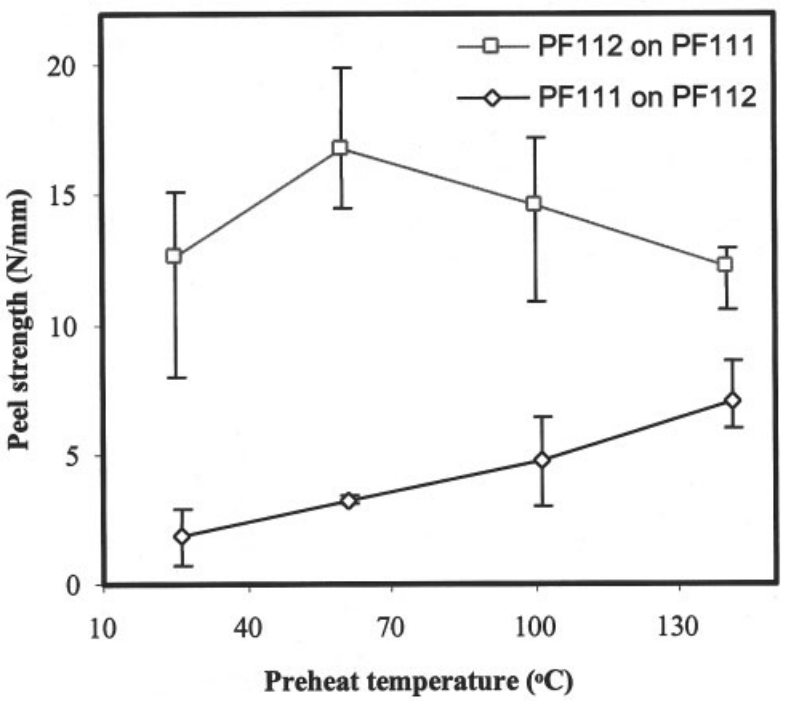

(b)

Figure 8 Peel strength of the bilayer coatings of (a) PF111 on PF111 and PF112 on PF112 and (b) mixed bilayers of PF111 on PF112 and PF112 on PF111 (first layer: PT = 100°C, FCT = 230°C; second layer: FCT = 230°C).

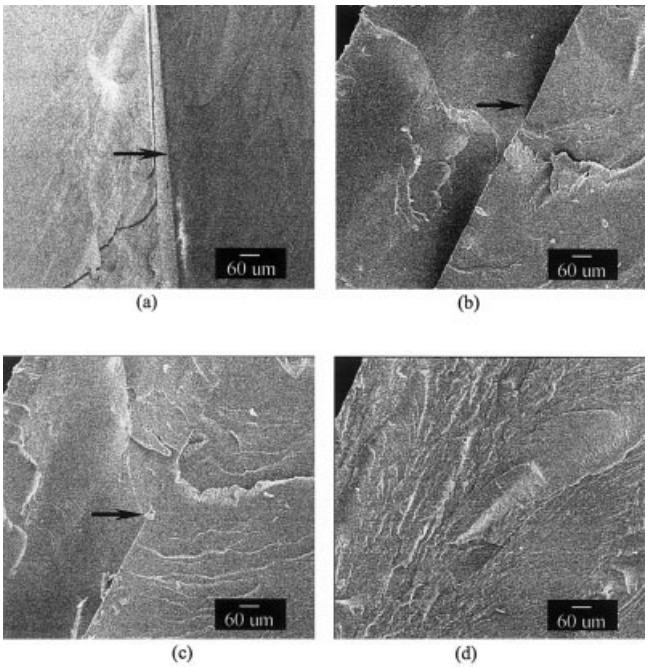

Figure 9 Cross-sections of the interface (shown with an arrow) in PF111 on PF112 bilayer coatings prepared at PTs (for the second layer) of (a) room temperature, (b) 60°C, (c) 100°C, and (d) 140°C (first layer: PT = 100°C, FCT = 230°C; second layer: FCT = 230°C).

Observation of the interfaces of the bilayer coatings

It was necessary for us to investigate the interfaces to understand the nature of the interactions between the polymer layers. For this purpose, the cross-sections of bilayer coatings were observed with SEM. Figure 9 depicts the interfaces of bilayer coatings formed under different PTs. The polymer–polymer interface existed, and the border was very clear for the sample at room temperature; however, an increase in PT produced a less discernible interface. For samples with a PT of 140°C, it was quite difficult to distinguish the interface, as shown in Figure 9. The first layer underwent a complex process of remelting, whereas the top layer underwent a more simple melting process. The complex thermal history might have caused a different stress distribution between polymer layers and may have been the prime reason why bilayer coatings always separated along the interface during the peeling process. The different stress distribution in the first layer could be distinguished from the fracture markings on the cross-section of bilayer coatings, as shown in Figure 10.

By observing the peeled surface of the coatings, we found that the adhesion of the second coating to the first coated surface was mainly due to the existence of many welding points. Figure 11(a) shows the surface features of an individual welding point on the peeled coating surface. The formation of weld points were

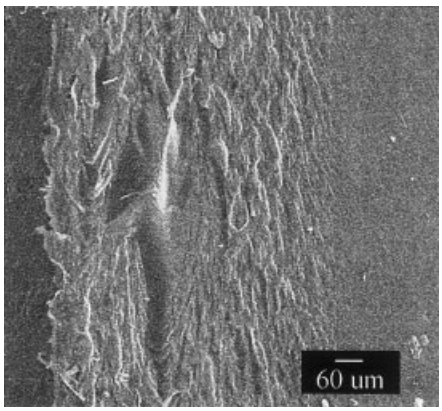

Figure 10 Cross-section of PF112 on PF111 bilayer coating (first layer: PT = 100°C, FCT = 230°C; second layer: PT = 140°C, FCT = 230°C).

attributed to the impact of molten particles onto the first layer. A higher PT of the first layer softened the base layer and promoted indiffusion. The stronger peel strength between coatings arose because of the existence of more weld points at the interface. Thus, a

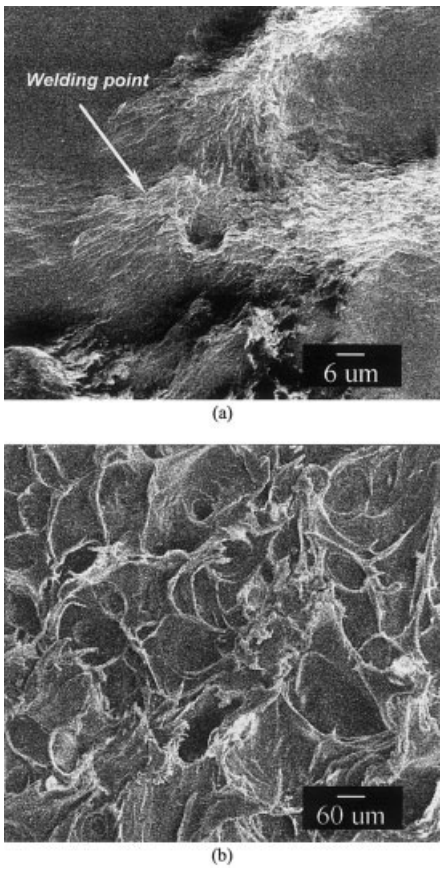

Figure 11 Peeled surface of a PF112 layer from a PF111 layer indicating (a) welding points when no preheat was employed on PF111 and (b) uniform bonding over the entire surface when a preheat of 60°C was used for the deposition of PF112 on PF111 (first layer: PT = 100°C, FCT = 230°C; second layer: FCT = 230°C).

layer exhibiting a greater cohesion produced a higher roughness on the peeled surface layer, as shown in Figure 11(b).

CONCLUSIONS

The thermal-spray process produced some crystallization of both the EMAA copolymer and ionomer feedstock powders. Density measurements indicated that the thermal-spray coating was porous, which was attributable to the formation mechanism of a sprayed coating and the degradation of polymer powder during the process schedule.

Tensile testing of coatings produced with a final temperature of 210–260°C yielded an increase in both the strains at fracture and the tensile strengths of PF111 and PF112 but led to a decrease in the 1% secant modulus.

The peel strength of monolayer coatings increased with PT of the underlying steel substrate, which arose from an increase in the contact area. The peel strength of the copolymer was higher than the ionomer because of a greater availability of molecules for secondary bonding of the methacrylic units.

The peel-strength test of bilayered coatings revealed that the interface cohesion of polymer to polymer was always stronger than that of polymer to steel. Furthermore, this strength increased with PT of the first polymer coating until a plateau was reached at the melting temperature. The cohesion was stronger with the ionomer than with the copolymer. Cohesion of the ionomer on the copolymer was significantly higher than that of the copolymer on the ionomer.

On the basis of SEM observation, we concluded that bilayer polymer coatings exhibited a visually detectable interface. Although the border formed under high preheating temperatures was not clear, it was still easily distinguished by the location of cracks on the cross-section of the bilayer coating. The welding points between the two polymer coatings, as observed in the SEM study, also provided evidence of the cohesion mechanism.

For industrial applications, a PT higher than the melting point of polymer should be used to achieve good adhesion. For repair, the use of an EMAA ionomer top-layer coating on a copolymer coating will provide the best coating integrity and adhesion results.

References

1. Lochner, K. H. Glass Sci Technol 1997, 70, 140.
2. Favre-Quattropani, L.; Groening, P.; Ramseyer, P.; Schlapbach, L. Surf Coat Technol 2000, 125, 377.
3. Kawase, R.; Nakano, A. Thermal Spray: Practical Solutions for Engineering Problems; ASM International: Materials Park, 1996; p 257.
4. Petrovicova, E.; Knight, R.; Schadler, L. S.; Twardowski, T. E. J Appl Polym Sci 2000, 78, 2272.
5. Lathabai, S.; Ottmuller, M.; Fernandez, I. Wear 1998, 221, 93.
6. Miller, R. A.; Rangaswamy, S.; Borel, M. A.; Vicoll, A. R. Thermal Spray Research & Applications; ASM International: 1990; p 125.
7. Tufa, K. Y.; Gitzhofer, F. Thermal Spray: The Challenges of the 21st Century; ASM International: Materials Park, 1998; p 157.
8. Herman, H.; Sampath, S.; McCune, R. MRS Bull 2000, 25, 17.
9. Fender, T. D. Mater Technol 1996, 11, 16.
10. van den Berge, F. M. J. Adv Mater Process 1998, 158, 31.
11. Parker, D. S. Plat Surf Eng 1995, 82, 20.
12. Grimenstein, L. Weld J 1995, 74, 53.
13. Heinrich, P.; Meinass, H.; Penszior, C. 5th High Velocity Spray Colloquium; Gemeinschaft Thermisches Spritzen: Unterschleissheim, Germany, 2000; p 65.
14. Brogan, J. A. MRS Bull 2000, 25, 48.
15. Kharitonov, V. V.; Yurkevich, O. R. J Eng Phys 1986, 50, 271.
16. Vardelle, A.; Moreau, C.; Fauchais, P. MRS Bull 2000, 25, 32.
17. Rollason, E. C.; Tumer, T. H.; Budgen, N. F. Metal Spraying: The Origin, Development, and Applications of the Metal-Spray Process of Metallisation with Special Reference to the Nature of Coatings; Griffin: London, 1939; p 196.
18. Anonymous. Ind Paint Powd 1994, 70, 31.
19. Xu, S.; Peng, H.; Qiang, G. Trans Inst Metal Finish 1997, 75, 70.
20. Zhang, T.; Gawne, D. T.; Bao, Y. Surf Coat Technol 1997, 96, 337.
21. Strait, L. H.; Jamison, R. D. J Comp Mater 1994, 28, 211.
22. MacKnight, W. J.; Kajiyama, T.; McKenna, L. Polym Eng Sci 1968, 8, 267.
23. Tsujita, Y.; Shibayama, K.; Takizawa, A.; Kinoshita, T. J Appl Polym Sci 1987, 33, 1307.
24. Kohzaki, M.; Tsujita, Y.; Takizawa, A.; Kinoshita, T. J Appl Polym Sci 1987, 33, 2393.
25. Brogan, J. A.; Berndt, C. C. J Mater Sci 1997, 32, 2099.
26. Brogan, J. A.; Berndt, C. C.; Simon, G. P.; Hewitt, D. Polym Eng Sci 1998, 38, 1873.
27. Brogan, J. A.; Berndt, C. C.; Claudon, A.; Coddet, C. Thermal Spray: Practical Solutions for Engineering Problems; ASM International: Materials Park, 1996; p 221.
28. Sun, L.; Berndt, C. C.; Gross, K. A. In Thermal Spray 2001: New Surfaces for a New Millennium; ASM International: Materials Park, 2001; p 321.
29. Gawne, D. T.; Zhang, T.; Bao, Y. In Thermal Spray 2001: New Surfaces for a New Millennium; ASM International: Materials Park, 2001; p 307.